Physics Letters B 718 (2012) 56–63

Contents lists available at SciVerse ScienceDirect

Physics Letters B

www.elsevier.com/locate/physletb

Measurement of angular correlations of jets at $\sqrt{s} = 1.96$ TeV and determination of the strong coupling at high momentum transfers

D0 Collaboration

V.M. Abazov [af], B. Abbott [bq], B.S. Acharya [z], M. Adams [at], T. Adams [ar], G.D. Alexeev [af], G. Alkhazov [aj], A. Alton [bf,1], G. Alverson [be], A. Askew [ar], S. Atkins [bc], K. Augsten [g], C. Avila [e], F. Badaud [j], L. Bagby [as], B. Baldin [as], D.V. Bandurin [ar], S. Banerjee [z], E. Barberis [be], P. Baringer [ba], J.F. Bartlett [as], U. Bassler [o], V. Bazterra [at], A. Bean [ba], M. Begalli [b], L. Bellantoni [as], S.B. Beri [x], G. Bernardi [n], R. Bernhard [s], I. Bertram [am], M. Besançon [o], R. Beuselinck [an], P.C. Bhat [as], S. Bhatia [bh], V. Bhatnagar [x], G. Blazey [au], S. Blessing [ar], K. Bloom [bi], A. Boehnlein [as], D. Boline [bn], E.E. Boos [ah], G. Borissov [am], T. Bose [bd], A. Brandt [bt], O. Brandt [t], R. Brock [bg], A. Bross [as], D. Brown [n], J. Brown [n], X.B. Bu [as], M. Buehler [as], V. Buescher [u], V. Bunichev [ah], S. Burdin [am,2], C.P. Buszello [al], E. Camacho-Pérez [ac], B.C.K. Casey [as], H. Castilla-Valdez [ac], S. Caughron [bg], S. Chakrabarti [bn], D. Chakraborty [au], K.M. Chan [ay], A. Chandra [bv], E. Chapon [o], G. Chen [ba], S. Chevalier-Théry [o], D.K. Cho [bs], S.W. Cho [ab], S. Choi [ab], B. Choudhary [y], S. Cihangir [as], D. Claes [bi], J. Clutter [ba], M. Cooke [as], W.E. Cooper [as], M. Corcoran [bv], F. Couderc [o], M.-C. Cousinou [l], A. Croc [o], D. Cutts [bs], A. Das [ap], G. Davies [an], S.J. de Jong [ad,ae], E. De La Cruz-Burelo [ac], F. Déliot [o], R. Demina [bm], D. Denisov [as], S.P. Denisov [ai], S. Desai [as], C. Deterre [o], K. DeVaughan [bi], H.T. Diehl [as], M. Diesburg [as], P.F. Ding [ao], A. Dominguez [bi], A. Dubey [y], L.V. Dudko [ah], D. Duggan [bj], A. Duperrin [l], S. Dutt [x], A. Dyshkant [au], M. Eads [bi], D. Edmunds [bg], J. Ellison [aq], V.D. Elvira [as], Y. Enari [n], H. Evans [aw], A. Evdokimov [bo], V.N. Evdokimov [ai], G. Facini [be], L. Feng [au], T. Ferbel [bm], F. Fiedler [u], F. Filthaut [ad,ae], W. Fisher [bg], H.E. Fisk [as], M. Fortner [au], H. Fox [am], S. Fuess [as], A. Garcia-Bellido [bm], J.A. García-González [ac], G.A. García-Guerra [ac,3], V. Gavrilov [ag], P. Gay [j], W. Geng [l,bg], D. Gerbaudo [bk], C.E. Gerber [at], Y. Gershtein [bj], G. Ginther [as,bm], G. Golovanov [af], A. Goussiou [bx], P.D. Grannis [bn], S. Greder [p], H. Greenlee [as], G. Grenier [q], Ph. Gris [j], J.-F. Grivaz [m], A. Grohsjean [o,4], S. Grünendahl [as], M.W. Grünewald [aa], T. Guillemin [m], G. Gutierrez [as], P. Gutierrez [bq], S. Hagopian [ar], J. Haley [be], L. Han [d], K. Harder [ao], A. Harel [bm], J.M. Hauptman [az], J. Hays [an], T. Head [ao], T. Hebbeker [r], D. Hedin [au], H. Hegab [br], A.P. Heinson [aq], U. Heintz [bs], C. Hensel [t], I. Heredia-De La Cruz [ac], K. Herner [bf], G. Hesketh [ao,6], M.D. Hildreth [ay], R. Hirosky [bw], T. Hoang [ar], J.D. Hobbs [bn], B. Hoeneisen [i], J. Hogan [bv], M. Hohlfeld [u], I. Howley [bt], Z. Hubacek [g,o], V. Hynek [g], I. Iashvili [bl], Y. Ilchenko [bu], R. Illingworth [as], A.S. Ito [as], S. Jabeen [bs], M. Jaffré [m], A. Jayasinghe [bq], M.S. Jeong [ab], R. Jesik [an], K. Johns [ap], E. Johnson [bg], M. Johnson [as], A. Jonckheere [as], P. Jonsson [an], J. Joshi [aq], A.W. Jung [as], A. Juste [ak], K. Kaadze [bb], E. Kajfasz [l], D. Karmanov [ah], P.A. Kasper [as], I. Katsanos [bi], R. Kehoe [bu], S. Kermiche [l], N. Khalatyan [as], A. Khanov [br], A. Kharchilava [bl], Y.N. Kharzheev [af], I. Kiselevich [ag], J.M. Kohli [x], A.V. Kozelov [ai], J. Kraus [bh], S. Kulikov [ai], A. Kumar [bl], A. Kupco [h], T. Kurča [q], V.A. Kuzmin [ah], S. Lammers [aw], G. Landsberg [bs], P. Lebrun [q], H.S. Lee [ab], S.W. Lee [az], W.M. Lee [as], X. Lei [ap], J. Lellouch [n], H. Li [k], L. Li [aq], Q.Z. Li [as], J.K. Lim [ab], D. Lincoln [as], J. Linnemann [bg], V.V. Lipaev [ai], R. Lipton [as], H. Liu [bu], Y. Liu [d], A. Lobodenko [aj], M. Lokajicek [h], R. Lopes de Sa [bn], H.J. Lubatti [bx], R. Luna-Garcia [ac,7], A.L. Lyon [as], A.K.A. Maciel [a], R. Madar [o], R. Magaña-Villalba [ac], S. Malik [bi], V.L. Malyshev [af], Y. Maravin [bb], J. Martínez-Ortega [ac], R. McCarthy [bn], C.L. McGivern [ao], M.M. Meijer [ad,ae], A. Melnitchouk [bh], D. Menezes [au], P.G. Mercadante [c], M. Merkin [ah], A. Meyer [r], J. Meyer [t], F. Miconi [p], N.K. Mondal [z], M. Mulhearn [bw], E. Nagy [l], M. Naimuddin [y], M. Narain [bs], R. Nayyar [ap], H.A. Neal [bf], J.P. Negret [e], P. Neustroev [aj], T. Nunnemann [v], J. Orduna [bv], N. Osman [l], J. Osta [ay], M. Padilla [aq], A. Pal [bt], N. Parashar [ax], V. Parihar [bs],

0370-2693/$ – see front matter
http://dx.doi.org/10.1016/j.physletb.2012.10.003

S.K. Park [ab], R. Partridge [bs,5], N. Parua [aw], A. Patwa [bo], B. Penning [as], M. Perfilov [ah], Y. Peters [ao], K. Petridis [ao], G. Petrillo [bm], P. Pétroff [m], M.-A. Pleier [bo], P.L.M. Podesta-Lerma [ac,8], V.M. Podstavkov [as], A.V. Popov [ai], M. Prewitt [bv], D. Price [aw], N. Prokopenko [ai], J. Qian [bf], A. Quadt [t], B. Quinn [bh], M.S. Rangel [a], K. Ranjan [y], P.N. Ratoff [am], I. Razumov [ai], P. Renkel [bu], I. Ripp-Baudot [p], F. Rizatdinova [br], M. Rominsky [as], A. Ross [am], C. Royon [o], P. Rubinov [as], R. Ruchti [ay], G. Sajot [k], P. Salcido [au], A. Sánchez-Hernández [ac], M.P. Sanders [v], A.S. Santos [a,9], G. Savage [as], L. Sawyer [bc], T. Scanlon [an], R.D. Schamberger [bn], Y. Scheglov [aj], H. Schellman [av], S. Schlobohm [bx], C. Schwanenberger [ao], R. Schwienhorst [bg], J. Sekaric [ba], H. Severini [bq], E. Shabalina [t], V. Shary [o], S. Shaw [bg], A.A. Shchukin [ai], R.K. Shivpuri [y], V. Simak [g], P. Skubic [bq], P. Slattery [bm], D. Smirnov [ay], K.J. Smith [bl], G.R. Snow [bi], J. Snow [bp], S. Snyder [bo], S. Söldner-Rembold [ao], L. Sonnenschein [r], K. Soustruznik [f], J. Stark [k], D.A. Stoyanova [ai], M. Strauss [bq], L. Suter [ao], P. Svoisky [bq], M. Takahashi [ao], M. Titov [o], V.V. Tokmenin [af], Y.-T. Tsai [bm], K. Tschann-Grimm [bn], D. Tsybychev [bn], B. Tuchming [o], C. Tully [bk], L. Uvarov [aj], S. Uvarov [aj], S. Uzunyan [au], R. Van Kooten [aw], W.M. van Leeuwen [ad], N. Varelas [at], E.W. Varnes [ap], I.A. Vasilyev [ai], P. Verdier [q], A.Y. Verkheev [af], L.S. Vertogradov [af], M. Verzocchi [as], M. Vesterinen [ao], D. Vilanova [o], P. Vokac [g], H.D. Wahl [ar], M.H.L.S. Wang [as], J. Warchol [ay], G. Watts [bx], M. Wayne [ay], J. Weichert [u], L. Welty-Rieger [av], A. White [bt], D. Wicke [w], M.R.J. Williams [am], G.W. Wilson [ba], M. Wobisch [bc], D.R. Wood [be], T.R. Wyatt [ao], Y. Xie [as], R. Yamada [as], S. Yang [d], W.-C. Yang [ao], T. Yasuda [as], Y.A. Yatsunenko [af], W. Ye [bn], Z. Ye [as], H. Yin [as], K. Yip [bo], S.W. Youn [as], J.M. Yu [bf], J. Zennamo [bl], T. Zhao [bx], T.G. Zhao [ao], B. Zhou [bf], J. Zhu [bf], M. Zielinski [bm], D. Zieminska [aw], L. Zivkovic [bs]

[a] *LAFEX, Centro Brasileiro de Pesquisas Físicas, Rio de Janeiro, Brazil*
[b] *Universidade do Estado do Rio de Janeiro, Rio de Janeiro, Brazil*
[c] *Universidade Federal do ABC, Santo André, Brazil*
[d] *University of Science and Technology of China, Hefei, People's Republic of China*
[e] *Universidad de los Andes, Bogotá, Colombia*
[f] *Charles University, Faculty of Mathematics and Physics, Center for Particle Physics, Prague, Czech Republic*
[g] *Czech Technical University in Prague, Prague, Czech Republic*
[h] *Center for Particle Physics, Institute of Physics, Academy of Sciences of the Czech Republic, Prague, Czech Republic*
[i] *Universidad San Francisco de Quito, Quito, Ecuador*
[j] *LPC, Université Blaise Pascal, CNRS/IN2P3, Clermont, France*
[k] *LPSC, Université Joseph Fourier Grenoble 1, CNRS/IN2P3, Institut National Polytechnique de Grenoble, Grenoble, France*
[l] *CPPM, Aix-Marseille Université, CNRS/IN2P3, Marseille, France*
[m] *LAL, Université Paris-Sud, CNRS/IN2P3, Orsay, France*
[n] *LPNHE, Universités Paris VI and VII, CNRS/IN2P3, Paris, France*
[o] *CEA, Irfu, SPP, Saclay, France*
[p] *IPHC, Université de Strasbourg, CNRS/IN2P3, Strasbourg, France*
[q] *IPNL, Université Lyon 1, CNRS/IN2P3, Villeurbanne, France and Université de Lyon, Lyon, France*
[r] *III. Physikalisches Institut A, RWTH Aachen University, Aachen, Germany*
[s] *Physikalisches Institut, Universität Freiburg, Freiburg, Germany*
[t] *II. Physikalisches Institut, Georg-August-Universität Göttingen, Göttingen, Germany*
[u] *Institut für Physik, Universität Mainz, Mainz, Germany*
[v] *Ludwig-Maximilians-Universität München, München, Germany*
[w] *Fachbereich Physik, Bergische Universität Wuppertal, Wuppertal, Germany*
[x] *Panjab University, Chandigarh, India*
[y] *Delhi University, Delhi, India*
[z] *Tata Institute of Fundamental Research, Mumbai, India*
[aa] *University College Dublin, Dublin, Ireland*
[ab] *Korea Detector Laboratory, Korea University, Seoul, Republic of Korea*
[ac] *CINVESTAV, Mexico City, Mexico*
[ad] *Nikhef, Science Park, Amsterdam, The Netherlands*
[ae] *Radboud University Nijmegen, Nijmegen, The Netherlands*
[af] *Joint Institute for Nuclear Research, Dubna, Russia*
[ag] *Institute for Theoretical and Experimental Physics, Moscow, Russia*
[ah] *Moscow State University, Moscow, Russia*
[ai] *Institute for High Energy Physics, Protvino, Russia*
[aj] *Petersburg Nuclear Physics Institute, St. Petersburg, Russia*
[ak] *Institució Catalana de Recerca i Estudis Avançats (ICREA) and Institut de Física d'Altes Energies (IFAE), Barcelona, Spain*
[al] *Uppsala University, Uppsala, Sweden*
[am] *Lancaster University, Lancaster LA1 4YB, United Kingdom*
[an] *Imperial College London, London SW7 2AZ, United Kingdom*
[ao] *The University of Manchester, Manchester M13 9PL, United Kingdom*
[ap] *University of Arizona, Tucson, AZ 85721, USA*
[aq] *University of California Riverside, Riverside, CA 92521, USA*
[ar] *Florida State University, Tallahassee, FL 32306, USA*
[as] *Fermi National Accelerator Laboratory, Batavia, IL 60510, USA*
[at] *University of Illinois at Chicago, Chicago, IL 60607, USA*
[au] *Northern Illinois University, DeKalb, IL 60115, USA*
[av] *Northwestern University, Evanston, IL 60208, USA*
[aw] *Indiana University, Bloomington, IN 47405, USA*
[ax] *Purdue University Calumet, Hammond, IN 46323, USA*
[ay] *University of Notre Dame, Notre Dame, IN 46556, USA*

[az] Iowa State University, Ames, IA 50011, USA
[ba] University of Kansas, Lawrence, KS 66045, USA
[bb] Kansas State University, Manhattan, KS 66506, USA
[bc] Louisiana Tech University, Ruston, LA 71272, USA
[bd] Boston University, Boston, MA 02215, USA
[be] Northeastern University, Boston, MA 02115, USA
[bf] University of Michigan, Ann Arbor, MI 48109, USA
[bg] Michigan State University, East Lansing, MI 48824, USA
[bh] University of Mississippi, University, MS 38677, USA
[bi] University of Nebraska, Lincoln, NE 68588, USA
[bj] Rutgers University, Piscataway, NJ 08855, USA
[bk] Princeton University, Princeton, NJ 08544, USA
[bl] State University of New York, Buffalo, NY 14260, USA
[bm] University of Rochester, Rochester, NY 14627, USA
[bn] State University of New York, Stony Brook, NY 11794, USA
[bo] Brookhaven National Laboratory, Upton, NY 11973, USA
[bp] Langston University, Langston, OK 73050, USA
[bq] University of Oklahoma, Norman, OK 73019, USA
[br] Oklahoma State University, Stillwater, OK 74078, USA
[bs] Brown University, Providence, RI 02912, USA
[bt] University of Texas, Arlington, TX 76019, USA
[bu] Southern Methodist University, Dallas, TX 75275, USA
[bv] Rice University, Houston, TX 77005, USA
[bw] University of Virginia, Charlottesville, VA 22901, USA
[bx] University of Washington, Seattle, WA 98195, USA

ARTICLE INFO

Article history:
Received 20 July 2012
Received in revised form 29 September 2012
Accepted 1 October 2012
Available online 4 October 2012
Editor: H. Weerts

ABSTRACT

We present a measurement of the average value of a new observable at hadron colliders that is sensitive to QCD dynamics and to the strong coupling constant, while being only weakly sensitive to parton distribution functions. The observable measures the angular correlations of jets and is defined as the number of neighboring jets above a given transverse momentum threshold which accompany a given jet within a given distance ΔR in the plane of rapidity and azimuthal angle. The ensemble average over all jets in an inclusive jet sample is measured and the results are presented as a function of transverse momentum of the inclusive jets, in different regions of ΔR and for different transverse momentum requirements for the neighboring jets. The measurement is based on a data set corresponding to an integrated luminosity of 0.7 fb^{-1} collected with the D0 detector at the Fermilab Tevatron Collider in $p\bar{p}$ collisions at $\sqrt{s} = 1.96$ TeV. The results are well described by a perturbative QCD calculation in next-to-leading order in the strong coupling constant, corrected for non-perturbative effects. From these results, we extract the strong coupling and test the QCD predictions for its running over a range of momentum transfers of 50–400 GeV.

Quantum chromodynamics (QCD) predicts that the strong force between quarks and gluons becomes weaker when probed at high momentum transfers, corresponding to small distances. This property, referred to as asymptotic freedom, is derived from the renormalization group equation (RGE) [1–3]. The RGE does not predict the value of the strong coupling α_s, but it describes the dependence of α_s on the renormalization scale μ_R, and therefore on the momentum transfer. Tests of perturbative QCD (pQCD) and the property of asymptotic freedom can be divided into tests of the validity of the RGE and determinations of the value of α_s. By convention, α_s values extracted from data at different momentum transfers are evolved to the common scale $\mu_R = M_Z$ to allow comparisons between experiments. The current world average value is $\alpha_s(M_Z) = 0.1184 \pm 0.0007$ [4]. The validity of the RGE is tested by studying the dependence of α_s on the momentum transfer. At present, the RGE predictions have been tested in deep-inelastic $e^{\pm}p$ scattering and in e^+e^- annihilation, where α_s results have been obtained for momentum transfers up to 208 GeV [4]. Attempts to extract α_s at higher momentum transfers have been carried out using inclusive jet cross section data in hadron–hadron collisions [5,6]. These analysis methods require parton distribution functions (PDFs) of the proton at large scales as input. Since the main constraints on PDFs come from data at lower scales, the knowledge of PDFs at large scales is mainly based on the evolution according to the Dokshitzer–Gribov–Lipatov–Altarelli–Parisi (DGLAP) evolution equations [7–9] which use α_s and the RGE as input. The α_s results from inclusive jet cross section data at high momentum transfers can therefore not be regarded as tests of the RGE, since they are obtained assuming its validity.

In this Letter a new observable for hadron–hadron collisions is introduced and its average value is measured. It is related to the angular correlations of jets. In pQCD, this quantity is computed as a ratio of jet cross sections, which is proportional to α_s. Since PDF dependencies largely cancel in the ratio, the extracted α_s results are almost independent of initial assumptions on the RGE. Values of α_s are extracted for momentum transfers between 50 and 400 GeV. These provide the first test of the RGE at momentum transfers above 208 GeV.

[1] Visitor from Augustana College, Sioux Falls, SD, USA.
[2] Visitor from The University of Liverpool, Liverpool, UK.
[3] Visitor from UPIITA–IPN, Mexico City, Mexico.
[4] Visitor from DESY, Hamburg, Germany.
[5] Visitor from SLAC, Menlo Park, CA, USA.
[6] Visitor from University College London, London, UK.
[7] Visitor from Centro de Investigacion en Computacion – IPN, Mexico City, Mexico.
[8] Visitor from ECFM, Universidad Autonoma de Sinaloa, Culiacán, Mexico.
[9] Visitor from Universidade Estadual Paulista, São Paulo, Brazil.

The analysis presented in this Letter studies the properties of multi-jet production based on an inclusive jet sample in $p\bar{p}$ collisions at $\sqrt{s} = 1.96$ TeV. While pQCD predictions for any cross section at a hadron collider depend on the PDFs, quantities with significantly reduced PDF sensitivity can be constructed. One class of such quantities is ratios of three-jet and dijet cross sections. Based on such ratios, one can exploit the high energy reach at hadron colliders to determine α_s and to test the predictions of the RGE at previously unexplored momentum scales. A new observable is introduced, which probes the angular correlations of jets in the plane of rapidity y [10] and azimuthal angle ϕ. This observable measures the number of neighboring jets that accompany a given jet with transverse momentum (p_T) with respect to the beam axis. The measured quantity $R_{\Delta R}$ is the ensemble average over all jets in an inclusive jet sample of this observable. The inclusive jet sample consists of all jets in a given data set, and these jets are hereafter referred to as "inclusive jets". The measured quantity is given by

$$R_{\Delta R}\big(p_T, \Delta R, p_{T\,\mathrm{min}}^{\mathrm{nbr}}\big) = \frac{\sum_{i=1}^{N_{\mathrm{jet}}(p_T)} N_{\mathrm{nbr}}^{(i)}(\Delta R, p_{T\,\mathrm{min}}^{\mathrm{nbr}})}{N_{\mathrm{jet}}(p_T)} \tag{1}$$

where $N_{\mathrm{jet}}(p_T)$ is the number of inclusive jets in a given inclusive jet p_T bin, and $N_{\mathrm{nbr}}^{(i)}(\Delta R, p_{T\,\mathrm{min}}^{\mathrm{nbr}})$ is the number of neighboring jets with transverse momenta greater than $p_{T\,\mathrm{min}}^{\mathrm{nbr}}$, separated from the i-th inclusive jet by a distance ΔR within a specified interval $\Delta R_{\mathrm{min}} < \Delta R < \Delta R_{\mathrm{max}}$ with $\Delta R \equiv \sqrt{(\Delta y)^2 + (\Delta\phi)^2}$. For $\Delta R < \pi$, only topologies with at least three jets contribute to the numerator of Eq. (1), in pQCD, and $R_{\Delta R}$ is computed at lowest order as a ratio of three-jet ($\mathcal{O}(\alpha_s^3)$) and inclusive jet cross sections ($\mathcal{O}(\alpha_s^2)$). This ratio is proportional to α_s.

This measurement is based on a data set corresponding to an integrated luminosity of 0.7 fb^{-1} collected with the D0 detector at the Fermilab Tevatron Collider. $R_{\Delta R}(p_T, \Delta R, p_{T\,\mathrm{min}}^{\mathrm{nbr}})$ is measured in an inclusive jet sample at central rapidities $|y| < 1$ for $p_T > 50$ GeV, defined by the Run II midpoint cone jet algorithm [11] with a cone of radius $R_{\mathrm{cone}} = 0.7$ in y and ϕ. It is measured triple differentially, as a function of inclusive jet p_T, for different $p_{T\,\mathrm{min}}^{\mathrm{nbr}}$, and in different ΔR regions. The $p_{T\,\mathrm{min}}^{\mathrm{nbr}}$ requirements are 30, 50, 70, or 90 GeV, respectively, and the different ΔR intervals are $1.4 < \Delta R < 1.8$, $1.8 < \Delta R < 2.2$, and $2.2 < \Delta R < 2.6$. For jets with $R_{\mathrm{cone}} = 0.7$, the lower limit of $\Delta R > 1.4$ ensures that a jet does not overlap with its neighboring jets. The upper limit on ΔR is smaller than π, so that contributing neighboring jets stem only from three- (or more) jet topologies. The lowest $p_{T\,\mathrm{min}}^{\mathrm{nbr}}$ requirement is chosen to ensure that the jet energy calibration and the jet p_T resolutions are well understood. The trigger efficiencies are high for jets with $p_T > 50$ GeV in the inclusive jet sample. The requirement of $|y| < 1$ implies that $(|y| + \Delta R) < 3.6$ over the whole analysis phase space. In this rapidity region jets are well-measured in the D0 detector. The data are corrected for experimental effects and are presented at the "particle level", which includes all stable particles as defined in Ref. [12].

A detailed description of the D0 detector can be found in Ref. [13]. The event selection, jet reconstruction, and jet energy and momentum correction follow closely those used in recent D0 measurements of inclusive jet, dijet and three-jet production rates [14–18]. Jets are reconstructed in the finely segmented liquid-argon/uranium calorimeter which covers most of the solid angle for polar angles of $1.7^\circ \lesssim \theta \lesssim 178.3^\circ$ [13]. For this measurement, events are triggered by jet triggers. Trigger efficiencies are studied as a function of jet p_T by comparing the inclusive jet cross section in data sets obtained by triggers with different p_T thresholds in regions where the trigger with lower threshold is fully efficient. The trigger with lowest p_T threshold is shown to be fully efficient by studying an event sample obtained independently with a muon trigger. In each inclusive jet p_T bin, events are taken from a single trigger which has an efficiency higher than 99%.

The position of the $p\bar{p}$ interaction is determined from the tracks reconstructed using data from the silicon detector and scintillating fiber tracker located inside a 2 T solenoidal magnet [13]. The position is required to be within 50 cm of the detector center in the coordinate along the beam axis, with at least three tracks pointing to it. These requirements discard (7–9)% of the events, depending on the trigger used. Contributions from cosmic ray events are suppressed by requiring the missing transverse momentum in an event to be less than 70% (50%) of the uncorrected leading jet p_T if the latter is below (above) 100 GeV. The efficiency of this requirement for signal is found to be $> 99.5\%$ [14,18]. Requirements on the characteristics of calorimeter shower shapes are used to suppress the remaining background due to electrons, photons, and detector noise that would otherwise mimic jets. The efficiency for the shower shape requirements is above 97.5%, and the fraction of background events is below 0.1% for all p_T, as determined from distributions in signal and in background-enriched event samples.

The jet four-momenta reconstructed from calorimeter energy depositions are then corrected, on average, for the response of the calorimeter, the net energy flow through the jet cone, additional energy from previous beam crossings, and multiple $p\bar{p}$ interactions in the same event, but not for muons and neutrinos [14,18,19]. The absolute energy calibration is determined from $Z \to e^+e^-$ events and the p_T imbalance in γ + jet events in the region $|y| < 0.4$. The extension to larger rapidities is derived from dijet events using a similar data-driven method. In addition, corrections in the range (2–4)% are applied that take into account the difference in calorimeter response due to the difference in the fractional contributions of quark and gluon-initiated jets in the dijet and the γ + jet event samples. These corrections are determined using jets simulated with the PYTHIA event generator [20] that have been passed through a GEANT-based detector simulation [21]. The total corrections of the jet four-momenta vary between 50% and 20% for jet p_T between 50 and 400 GeV. An additional correction is applied for systematic shifts in $|y|$ due to detector effects [14,18]. These corrections adjust the reconstructed jet energy to the energy of the stable particles that enter the calorimeter except for muons and neutrinos.

The differential distributions $R_{\Delta R}(p_T, \Delta R, p_{T\,\mathrm{min}}^{\mathrm{nbr}})$ are corrected for experimental effects. Particle-level events are generated with SHERPA 1.1.3 [22] with MSTW2008LO PDFs [23] and with PYTHIA 6.419 [20] with CTEQ6.6 PDFs [24] and tune QW [25]. The jets from these events are processed by a fast simulation of the D0 detector response. The simulation is based on parameterizations of jet p_T resolutions and jet reconstruction efficiencies determined from data and of resolutions of the polar and azimuthal angles of jets, which are obtained from a detailed simulation of the detector using GEANT.

The p_T resolution for jets is about 15% at 40 GeV, decreasing to less than 10% at 400 GeV. To use the fast simulation to correct for experimental effects, the simulation must describe all relevant distributions, including the p_T, y and ΔR distributions for the inclusive jets and the neighboring jets. The generated events are reweighted, based on the properties of the generated jets, to match these distributions in data. To minimize migrations between inclusive jet p_T bins due to resolution effects, we use the simulation to obtain a rescaling function in reconstructed p_T that optimizes the correlation between the reconstructed and true values. The bin sizes in the p_T distributions are chosen to be approximately twice the p_T resolution. The bin purity after p_T rescaling, defined as the fraction of all reconstructed events that were generated in the same bin, is above 50% for all bins. We then use

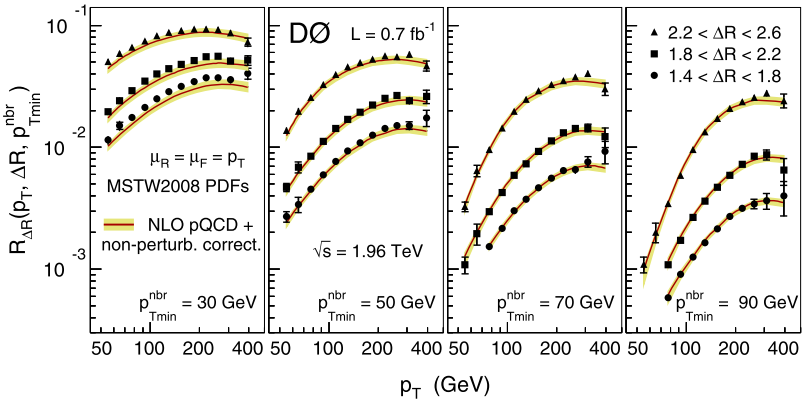

Fig. 1. (Color online.) The measurement of $R_{\Delta R}$ as a function of inclusive jet p_T for three different intervals in ΔR and for four different requirements of $p_{T\,\mathrm{min}}^{\mathrm{nbr}}$. The inner uncertainty bars indicate the statistical uncertainties, and the total uncertainty bars display the quadratic sum of the statistical and systematic uncertainties. The theory predictions are shown with their uncertainties.

the simulation to determine bin correction factors for experimental effects for all analysis bins. The correction factors are computed bin-by-bin as the ratio of $R_{\Delta R}$ without and with simulation of the detector response. These also include corrections for the energies of unreconstructed muons and neutrinos inside the jets. The total correction factors for $R_{\Delta R}$ using the reweighted PYTHIA and SHERPA simulations agree typically within 2%. The average factors, used to correct the data, are typically between 0.98 and 1.01, but never below 0.93 or above 1.03. The difference between the average and the individual corrections is taken into account as an uncertainty which is split into two contributions. One contribution corresponds to the systematic difference between the two individual corrections, and the other one corresponds to the statistical fluctuations. The former is attributed to the model dependence and assumed to be correlated between the data points, while the latter is included in the statistical uncertainty of the results.

In total, 69 independent sources of experimental systematic uncertainties are identified, mostly related to jet energy calibration and jet p_T resolution. The effects of each source are taken as fully correlated between all data points. The dominant uncertainties for the differential cross sections are due to the jet energy calibration (2–5)%, and the model dependence of the correction factors (2–3)%. Smaller contributions come from the jet p_T resolution (0.5–1.5)%, the jet ϕ resolution (0.5–2)%, and from the uncertainties in systematic shifts in y (0.5–1)%. All other sources are negligible. The total systematic uncertainties are between 2% and 6%.

The results for $R_{\Delta R}(p_T, \Delta R, p_{T\,\mathrm{min}}^{\mathrm{nbr}})$ are displayed in Fig. 1 as a function of inclusive jet p_T, in different regions of ΔR and for different $p_{T\,\mathrm{min}}^{\mathrm{nbr}}$. The values of p_T at which the data points are presented correspond to the geometric bin centers. A detailed documentation of the results, including the individual uncertainty contributions, is provided in the supplementary material. For a given ΔR region, and $p_{T\,\mathrm{min}}^{\mathrm{nbr}}$, $R_{\Delta R}$ increases with p_T up to a maximum value, above which it falls when approaching the kinematic limit. At fixed p_T, $R_{\Delta R}$ increases with ΔR and decreases with increasing $p_{T\,\mathrm{min}}^{\mathrm{nbr}}$. At lower p_T, $R_{\Delta R}$ depends more strongly on $p_{T\,\mathrm{min}}^{\mathrm{nbr}}$. For larger $p_{T\,\mathrm{min}}^{\mathrm{nbr}}$, both the p_T and the ΔR dependencies are stronger.

The theory predictions for $R_{\Delta R}$ which are compared to the data, and which are later used to extract α_s, are given by the product of the NLO pQCD results and correction factors for non-perturbative effects, including hadronization and underlying event. The non-perturbative corrections are determined using PYTHIA 6.425 with tunes AMBT1 [26] and DW [27], which use different parton shower and underlying event models. The hadronization correction is obtained from the ratio of $R_{\Delta R}$ at the parton level (after the parton shower) and the particle level (including all stable particles), both without underlying event. The underlying event correction is computed from the ratio of $R_{\Delta R}$ computed at the particle level with and without underlying event. The total corrections are defined as the combination of the corrections due to hadronization and the underlying event and they vary between +10% and −3% for tune AMBT1 and between −1% and −10% for tune DW. The results obtained with the two tunes agree typically within (2–4)% and always within 11%. The central results are taken to be the average values, and the uncertainty is taken to be half of the difference (given in the supplementary material). As a cross-check, the non-perturbative corrections have also been derived with HERWIG 6.520 [28,29]. The HERWIG results are consistent with the results from the PYTHIA tunes AMBT1 and DW for all kinematic regions considered in this analysis.

The NLO pQCD prediction is given by the ratio of an inclusive three-jet cross section and the inclusive jet cross section both evaluated at their respective NLO. The numerator and the denominator both depend on the PDFs and most of the PDF dependencies cancel in the ratio. A residual PDF dependence remains, due to small differences in the decomposition of the partonic subprocesses and a slightly different coverage of proton momentum fractions x in the numerator and the denominator. While the PDFs have no explicit α_s dependence, their knowledge (i.e. PDF parameterizations) depends implicitly on α_s due to assumptions on α_s during the extraction procedure. Therefore, the pQCD prediction for $R_{\Delta R}$ has an explicit α_s dependence stemming from the ratios of three-jet and inclusive jet matrix elements, and an implicit α_s dependence due to the residual dependence on the PDFs.

The NLO pQCD results are computed using FASTNLO [30] based on NLOJET++ [31,32], in the $\overline{\mathrm{MS}}$ scheme [33] for five active quark flavors. The calculations use the next-to-leading logarithmic (two-loop) approximation of the RGE and $\alpha_s(M_Z) = 0.118$ in the matrix elements and the PDFs, which is close to the current world average value of 0.1184 [4]. The central choice μ_0 for the renormalization and factorization scales is the inclusive jet p_T, $\mu_R = \mu_F = \mu_0 = p_T$, and the MSTW2008NLO PDFs [23] are used.

The uncertainties of the pQCD calculations due to uncalculated higher order contributions are estimated from the $\mu_{R,F}$ dependence. These are computed as the relative changes of the results due to independent variations of both scales between $\mu_0/2$ and $2\mu_0$, with the restriction of $0.5 \leqslant \mu_R/\mu_F \leqslant 2.0$. These variations affect the theory results by (3–9)%. The PDF uncertainties are computed using the up and down variations of the 20 orthogonal PDF uncertainty eigenvectors, corresponding to the 68% C.L., as provided by MSTW2008NLO. The $R_{\Delta R}$ results obtained with the CT10 [34] and NNPDFv2.1 [35] PDF parameterizations agree

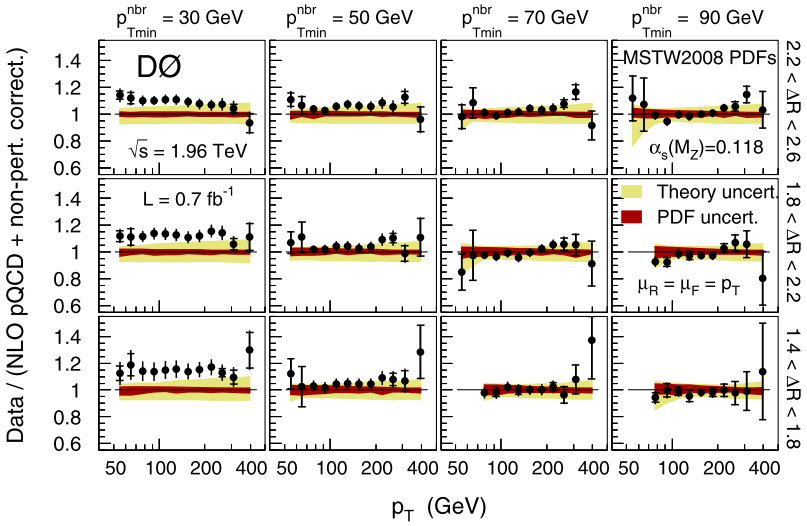

Fig. 2. (Color online.) The ratios of the $R_{\Delta R}$ measurements and the theory predictions obtained for MSTW2008NLO PDFs and $\alpha_s(M_Z) = 0.118$. The ratios are shown as a function of inclusive jet p_T in different regions of ΔR (rows) and for different $p_{T\,\mathrm{min}}^{\mathrm{nbr}}$ requirements (columns). The inner uncertainty bars indicate the statistical uncertainties, and the total uncertainty bars display the quadratic sum of the statistical and systematic uncertainties. The theory uncertainty is the quadratic sum of PDF and scale uncertainties.

with those for MSTW2008NLO typically within 1% and always within 3%.

The theory results are compared to the data in Fig. 1, and the ratios of data and theory are displayed in Fig. 2 for all twelve kinematic regions in ΔR and $p_{T\,\mathrm{min}}^{\mathrm{nbr}}$. The PDF uncertainties are (2–5)% and the scale uncertainties are typically (4–8)%. For higher $p_{T\,\mathrm{min}}^{\mathrm{nbr}} = 50$, 70, and 90 GeV, the theoretical predictions are in good agreement with data and the ratios are independent of p_T, ΔR, and $p_{T\,\mathrm{min}}^{\mathrm{nbr}}$. Only for $p_{T\,\mathrm{min}}^{\mathrm{nbr}} = 30$ GeV, the predictions are systematically below the data by (8–15)%. This might be caused by limitations of either the perturbative calculation or the modeling of the non-perturbative effects at low $p_{T\,\mathrm{min}}^{\mathrm{nbr}}$.

These $R_{\Delta R}$ results are then used to determine α_s and to test the two-loop RGE prediction for its running as a function of the scale p_T. In an initial study, the data are split into 12 subsets defined by the different $(\Delta R, p_{T\,\mathrm{min}}^{\mathrm{nbr}})$ requirements. Assuming the RGE, the value of $\alpha_s(M_Z)$ is fitted to each of these subsets, and the corresponding χ^2 values are determined that compare data and theory. Since each of these subsets covers a large inclusive jet p_T range, a violation of the RGE would be reflected in poor χ^2 values. Furthermore, the comparison of the extracted $\alpha_s(M_Z)$ values allows the study of the dependence of the results on ΔR and/or $p_{T\,\mathrm{min}}^{\mathrm{nbr}}$. The data from kinematic regions in $(\Delta R, p_{T\,\mathrm{min}}^{\mathrm{nbr}})$ in which the $\alpha_s(M_Z)$ fit results are consistent with each other are then used in the subsequent analysis. These data are split into 12 groups, each with the same inclusive jet p_T, combining data points for different $(\Delta R, p_{T\,\mathrm{min}}^{\mathrm{nbr}})$. For each group, α_s is determined at the corresponding p_T, and then evolved, using the RGE, to $\mu_R = M_Z$.

The α_s extraction requires the theory predictions to be available as a continuous function of α_s used in the matrix elements and PDFs. The global PDF fits [23,34,35] do not provide the full α_s dependence of their results, but only PDF sets at discrete values of $\alpha_s(M_Z)$, in increments of $\Delta\alpha_s(M_Z) = 0.001$. A continuous $\alpha_s(M_Z)$ dependence for $R_{\Delta R}$ is obtained, by cubic interpolation (linear extrapolation) of the theory results inside (outside) the available $\alpha_s(M_Z)$ range. For the central results, we use MSTW2008NLO PDFs which cover the largest range of $0.110 \leqslant \alpha_s(M_Z) \leqslant 0.130$. The fits determine α_s by using MINUIT [36] to minimize the χ^2 function [37] calculated from the differences between theory and data. All correlated systematic experimental and theoretical uncertainties are treated in the Hessian approach [37], except for the uncertainty due to the $\mu_{R,F}$ dependence. The correlated statistical uncertainties are taken into account via the covariance matrix. The α_s results are obtained by minimizing χ^2 with respect to α_s and the nuisance parameters for the correlated uncertainties. By scanning χ^2 as a function of α_s, the uncertainties are obtained from those α_s values for which χ^2 is increased by one with respect to the minimum value. Fits, that determine $\alpha_s(M_Z)$ use the two-loop solution of the RGE to translate $\alpha_s(M_Z)$ values to the corresponding values of $\alpha_s(p_T)$ which enter the pQCD calculations for the different p_T bins. These $\alpha_s(M_Z)$ results are therefore derived assuming the validity of the RGE. Those fits that extract $\alpha_s(p_T)$ from a group of data points in the same p_T bin are almost independent of the RGE. A small dependence on the RGE enters only due to the residual dependence of the $R_{\Delta R}$ predictions on the PDFs which use the RGE in their DGLAP evolution. Otherwise these $\alpha_s(p_T)$ fit results are independent of the RGE.

In the α_s determination, we consider the correlations of the statistical uncertainties and all 69 sources of correlated experimental systematic uncertainties. The theory uncertainties include the uncertainties of the non-perturbative corrections, the PDF uncertainties and the $\mu_{R,F}$ dependence of the pQCD calculations. Following Refs. [38–40], the uncertainty due to the $\mu_{R,F}$ dependence is computed by repeating the α_s fit for different choices of $\mu_{R,F}$ and the largest difference to the central result (obtained for $\mu_{R,F} = p_T$) is taken to be the corresponding uncertainty for α_s. The α_s fits are also repeated for CT10 and NNPDFv2.1 PDFs, and the largest differences are quoted as "PDF set" uncertainty. The uncertainties from the scale variation and from the different PDF sets are added in quadrature to the other uncertainties to obtain the total uncertainty.

Before the central α_s results are obtained, the consistency of the individual results for the 12 different $(\Delta R, p_{T\,\mathrm{min}}^{\mathrm{nbr}})$ regions, listed in Table 1, is tested. Assuming the RGE, the values of $\alpha_s(M_Z)$ are fitted to each of the 12 subsets, and listed in Table 1 together with the corresponding χ^2 values. All χ^2 values are consistent with the expectations based on the number of degrees of freedom (N_{dof}), $\chi^2 = N_{\mathrm{dof}} \pm \sqrt{2N_{\mathrm{dof}}}$. This means that the RGE is consistent with the observed p_T dependence of $\alpha_s(p_T)$ over the studied p_T range in all ΔR regions and for all $p_{T\,\mathrm{min}}^{\mathrm{nbr}}$. For the same $p_{T\,\mathrm{min}}^{\mathrm{nbr}}$, the $\alpha_s(M_Z)$ results for different ΔR regions are consistent with each other, i.e. there is no ΔR dependence. The $\alpha_s(M_Z)$ results are

Table 1
The $\alpha_s(M_Z)$ results with their absolute uncertainties and the χ^2 values from the fits to the $R_{\Delta R}$ data in each of the 12 kinematic regions, defined by the $p_{T\,\mathrm{min}}^{\mathrm{nbr}}$ and ΔR requirements.

$p_{T\,\mathrm{min}}^{\mathrm{nbr}}$	ΔR	$\alpha_s(M_Z)$	Total uncertainty		χ^2/N_{dof}
30 GeV	1.4–1.8	0.1290	+0.0073	−0.0078	6.9/11
30 GeV	1.8–2.2	0.1276	+0.0078	−0.0049	12.6/11
30 GeV	2.2–2.6	0.1249	+0.0133	−0.0020	15.3/11
50 GeV	1.4–1.8	0.1197	+0.0089	−0.0061	7.3/11
50 GeV	1.8–2.2	0.1168	+0.0083	−0.0039	14.1/11
50 GeV	2.2–2.6	0.1193	+0.0076	−0.0043	13.7/11
70 GeV	1.4–1.8	0.1168	+0.0101	−0.0073	4.9/9
70 GeV	1.8–2.2	0.1132	+0.0069	−0.0047	12.1/11
70 GeV	2.2–2.6	0.1156	+0.0080	−0.0039	16.8/11
90 GeV	1.4–1.8	0.1135	+0.0084	−0.0087	1.2/9
90 GeV	1.8–2.2	0.1136	+0.0067	−0.0069	9.7/9
90 GeV	2.2–2.6	0.1166	+0.0099	−0.0083	17.3/11

rather independent of $p_{T\,\mathrm{min}}^{\mathrm{nbr}}$ for $p_{T\,\mathrm{min}}^{\mathrm{nbr}} \geqslant 50$ GeV. Only the $\alpha_s(M_Z)$ results for the lowest requirement, $p_{T\,\mathrm{min}}^{\mathrm{nbr}} = 30$ GeV, are significantly higher. As mentioned earlier, at lowest $p_{T\,\mathrm{min}}^{\mathrm{nbr}}$ limitations of the perturbative calculations or the non-perturbative models may become visible. The data with $p_{T\,\mathrm{min}}^{\mathrm{nbr}} = 30$ GeV are therefore excluded when the final results of this analysis are determined.

All remaining data points with the same p_T (from all three ΔR regions and for $p_{T\,\mathrm{min}}^{\mathrm{nbr}} = 50$, 70, and 90 GeV) are combined to fit $\alpha_s(p_T)$, at the p_T value corresponding to the geometric center of the bin. This is done for all 12 different p_T bins in the range $50 < p_T < 450$ GeV and the results are listed in Table 2 and displayed in Fig. 3(a). Using the RGE, the individual results are then evolved to $\mu_R = M_Z$, and shown in Fig. 3(b). These α_s results from $R_{\Delta R}$, extracted using NLO pQCD, are in good agreement with our previous results from inclusive jet cross section data [38], extracted using NLO plus 2-loop contributions from threshold corrections [42], and with the results from a reanalysis of event shape data from the ALEPH experiment at the LEP e^+e^- collider, extracted using NNLO calculations [41]. A combined fit, using the same data set integrated over p_T, and for MSTW2008NLO PDFs, gives the $\alpha_s(M_Z)$ result listed in Table 3. The results obtained for CT10 PDFs ($\alpha_s(M_Z) = 0.1189$) and NNPDFv2.1 ($\alpha_s(M_Z) = 0.1167$) are used to define the uncertainty due to the PDF set. This result is in good agreement with our previous result of $\alpha_s(M_Z) = 0.1161^{+0.0041}_{-0.0048}$, obtained from inclusive jet cross section data at $p_T < 145$ GeV [5], and the world average value [4].

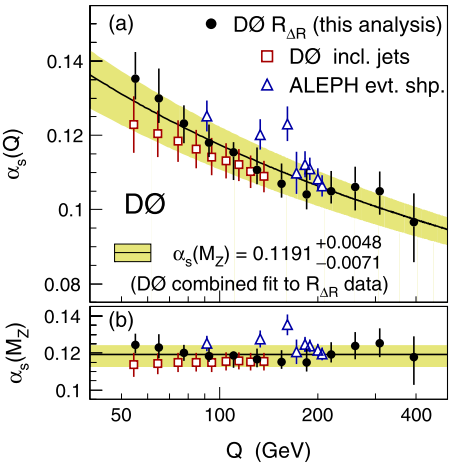

Fig. 3. (Color online.) The strong coupling α_s at large momentum transfers, Q, presented as $\alpha_s(Q)$ (a) and evolved to M_Z using the RGE (b). The uncertainty bars indicate the total uncertainty, including the experimental and theoretical contributions. The new α_s results from $R_{\Delta R}$ are compared to previous results obtained from inclusive jet cross section data [38] and from event shape data [41]. The $\alpha_s(M_Z)$ result from the combined fit to all selected data points (b) and the corresponding RGE prediction (a) are also shown.

The RGE prediction for this result is displayed in Fig. 3(a). The new $\alpha_s(p_T)$ results from $R_{\Delta R}$ are well described by the RGE prediction including the region $208 < \mu_R < 400$ GeV, in which the RGE is tested for the first time.

In summary, a measurement has been presented of a new quantity $R_{\Delta R}$ which probes the angular correlations of jets. $R_{\Delta R}$ is measured as a function of inclusive jet p_T in different annular regions of ΔR between a jet and its neighboring jets and for different requirements on the minimal transverse momentum of the neighboring jet $p_{T\,\mathrm{min}}^{\mathrm{nbr}}$. The data for $p_T > 50$ GeV are well-described by pQCD calculations in NLO in α_s with non-perturbative corrections applied. Results for $\alpha_s(p_T)$ are extracted using the data with $p_{T\,\mathrm{min}}^{\mathrm{nbr}} \geqslant 50$ GeV, integrated over ΔR. The extracted $\alpha_s(p_T)$ results from $R_{\Delta R}$ are, to good approximation, independent of the PDFs and thus independent of assumptions on the RGE. Therefore, these α_s results are the first to provide a test of the RGE at momentum transfers beyond 208 GeV. The results are in good agreement with previous results and consistent with the RGE predictions for the running of α_s for momentum trans-

Table 2
Central values and uncertainties due to different sources for the 12 $\alpha_s(p_T)$ results obtained by combining the data at the same p_T from all ΔR regions for $p_{T\,\mathrm{min}}^{\mathrm{nbr}} = 50$, 70, and 90 GeV. All uncertainties are multiplied by a factor of 10^3.

p_T range (GeV)	p_T (GeV)	$\alpha_s(p_T)$	Total uncertainty	Statistical	Experimental correlated	Non-perturbative corrections	MSTW2008NLO uncertainty	PDF set	$\mu_{R,F}$ variation
50–60	55.0	0.1353	$^{+7.2}_{-5.6}$	±2.8	$^{+2.6}_{-2.8}$	$^{+2.5}_{-2.8}$	$^{+1.3}_{-1.2}$	$^{+0.2}_{-0.4}$	$^{+5.4}_{-0.8}$
60–70	65.0	0.1299	$^{+8.1}_{-6.6}$	±4.2	$^{+2.3}_{-2.7}$	$^{+2.1}_{-2.4}$	$^{+1.2}_{-1.4}$	$^{+0.3}_{-1.3}$	$^{+6.1}_{-1.5}$
70–85	77.5	0.1232	$^{+4.9}_{-5.3}$	±0.6	$^{+1.6}_{-3.2}$	$^{+1.4}_{-1.0}$	$^{+1.9}_{-1.0}$	$^{+1.8}_{-0.9}$	$^{+3.5}_{-3.9}$
85–100	92.5	0.1180	$^{+4.9}_{-3.8}$	±0.8	$^{+2.8}_{-2.4}$	$^{+1.0}_{-2.2}$	$^{+2.1}_{-1.1}$	$^{+1.0}_{-0.0}$	$^{+3.0}_{-1.4}$
100–120	110	0.1154	$^{+2.8}_{-7.4}$	±0.6	$^{+2.1}_{-2.4}$	$^{+0.3}_{-0.4}$	$^{+1.0}_{-5.0}$	$^{+0.0}_{-3.7}$	$^{+1.4}_{-3.1}$
120–140	130	0.1107	$^{+6.0}_{-3.9}$	±0.6	$^{+2.8}_{-2.2}$	$^{+0.4}_{-0.4}$	$^{+1.5}_{-2.5}$	$^{+2.0}_{-0.0}$	$^{+4.7}_{-1.9}$
140–170	155	0.1070	$^{+5.4}_{-3.8}$	±0.5	$^{+1.6}_{-3.0}$	$^{+0.1}_{-0.3}$	$^{+0.9}_{-0.8}$	$^{+1.5}_{-0.0}$	$^{+4.9}_{-2.2}$
170–200	185	0.1041	$^{+6.7}_{-4.0}$	±0.5	$^{+2.5}_{-2.1}$	$^{+0.7}_{-0.4}$	$^{+0.3}_{-1.5}$	$^{+3.0}_{-0.0}$	$^{+5.4}_{-2.9}$
200–240	220	0.1050	$^{+5.4}_{-3.3}$	±0.3	$^{+2.5}_{-2.3}$	$^{+0.6}_{-0.3}$	$^{+1.0}_{-0.2}$	$^{+0.8}_{-0.6}$	$^{+4.5}_{-2.3}$
240–280	260	0.1061	$^{+5.5}_{-6.3}$	±0.6	$^{+1.0}_{-3.2}$	$^{+1.0}_{-0.8}$	$^{+0.3}_{-0.7}$	$^{+0.0}_{-3.3}$	$^{+5.3}_{-4.2}$
280–340	310	0.1049	$^{+5.4}_{-6.2}$	±1.0	$^{+1.6}_{-2.3}$	$^{+0.4}_{-0.3}$	$^{+0.3}_{-0.6}$	$^{+0.6}_{-3.3}$	$^{+5.0}_{-4.3}$
340–450	395	0.0966	$^{+7.8}_{-10.8}$	±5.4	$^{+1.9}_{-5.9}$	$^{+0.1}_{-1.0}$	$^{+0.2}_{-0.9}$	$^{+0.0}_{-3.3}$	$^{+5.3}_{-4.7}$

Table 3
The $\alpha_s(M_Z)$ result for $R_{\Delta R}$, obtained by combining all data points in p_T and in ΔR for the requirements $p_{T\,\mathrm{min}}^{\mathrm{nbr}} = 50$, 70, and 90 GeV. All uncertainties are multiplied by a factor of 10^3.

$\alpha_s(M_Z)$	Total uncertainty	Statistical	Experimental correlated	Non-perturbative corrections	MSTW2008NLO uncertainty	PDF set	$\mu_{R,F}$ variation
0.1191	$^{+4.8}_{-7.1}$	± 0.3	$^{+0.7}_{-0.9}$	$^{+0.2}_{-0.1}$	$^{+1.0}_{-0.5}$	$^{+0.0}_{-2.4}$	$^{+4.6}_{-6.6}$

fers up to 400 GeV. The combined $\alpha_s(M_Z)$ result, obtained using the data with $p_{T\,\mathrm{min}}^{\mathrm{nbr}} \geqslant 50$ GeV (integrated over ΔR and p_T), is $\alpha_s(M_Z) = 0.1191^{+0.0048}_{-0.0071}$, in good agreement with the world average value [4].

Acknowledgements

We thank the staffs at Fermilab and collaborating institutions, and acknowledge support from the DOE and NSF (USA); CEA and CNRS/IN2P3 (France); MON, NRC KI and RFBR (Russia); CNPq, FAPERJ, FAPESP and FUNDUNESP (Brazil); DAE and DST (India); Colciencias (Colombia); CONACyT (Mexico); NRF (Korea); FOM (The Netherlands); STFC and the Royal Society (United Kingdom); MSMT and GACR (Czech Republic); BMBF and DFG (Germany); SFI (Ireland); The Swedish Research Council (Sweden); and CAS and CNSF (China).

Appendix A. Supplementary material

Supplementary material related to this Letter can be found online at http://dx.doi.org/10.1016/j.physletb.2012.10.003.

References

[1] C.G. Callan Jr., Phys. Rev. D 2 (1970) 1541.
[2] K. Symanzik, Commun. Math. Phys. 18 (1970) 227.
[3] K. Symanzik, Commun. Math. Phys. 23 (1971) 49.
[4] J. Beringer, et al., Particle Data Group, Phys. Rev. D 86 (2012) 010001, and references therein.
[5] A.A. Affolder, et al., CDF Collaboration, Phys. Rev. Lett. 88 (2002) 042001.
[6] B. Malaescu, P. Starovoitov, Eur. Phys. J. C 72 (2012) 2041.
[7] V.N. Gribov, L.N. Lipatov, Sov. J. Nucl. Phys. 15 (1972) 438, Yad. Fiz. 15 (1972) 781.
[8] G. Altarelli, G. Parisi, Nucl. Phys. B 126 (1977) 298.
[9] Y.L. Dokshitzer, Sov. Phys. JETP 46 (1977) 641, Zh. Eksp. Teor. Fiz. 73 (1977) 1216.
[10] Rapidity y is related to the polar scattering angle θ with respect to the proton beam axis by $y = \frac{1}{2}\ln[(1+\beta\cos\theta)/(1-\beta\cos\theta)]$, where β is defined as the ratio of the magnitude of the momentum and energy, $\beta = |\vec{p}|/E$.
[11] G.C. Blazey, et al., in: U. Baur, R.K. Ellis, D. Zeppenfeld (Eds.), Proceedings of the Workshop: QCD and Weak Boson Physics in Run II, Fermilab-Pub-00/297, 2000.
[12] C. Buttar, et al., in: G. Belanger, et al. (Eds.), Les Houches 2007, Physics at TeV Colliders, arXiv:0803.0678 [hep-ph], Section 9.
[13] V.M. Abazov, et al., D0 Collaboration, Nucl. Instrum. Methods Phys. Res. A 565 (2006) 463.
[14] V.M. Abazov, et al., D0 Collaboration, Phys. Rev. Lett. 101 (2008) 062001.
[15] V.M. Abazov, et al., D0 Collaboration, Phys. Rev. Lett. 103 (2009) 191803.
[16] V.M. Abazov, et al., D0 Collaboration, Phys. Lett. B 693 (2010) 531.
[17] V.M. Abazov, et al., D0 Collaboration, Phys. Lett. B 704 (2011) 434.
[18] V.M. Abazov, et al., D0 Collaboration, Phys. Rev. D 85 (2012) 052006.
[19] M. Voutilainen, Fermilab-Thesis-2008-19, 2008.
[20] T. Sjöstrand, et al., Comput. Phys. Commun. 135 (2001) 238.
[21] R. Brun, F. Carminati, CERN Program Library Long Writeup W5013, 1993.
[22] T. Gleisberg, et al., J. High Energy Phys. 0902 (2009) 007.
[23] A.D. Martin, et al., Eur. Phys. J. C 63 (2009) 189.
[24] P.M. Nadolsky, et al., Phys. Rev. D 78 (2008) 013004.
[25] T.Q.W. Group, et al., arXiv:hep-ph/0610012.
[26] G. Brandt, in: M. Diehl, J. Haller, T. Schorner-Sadenius, G. Steinbruck (Eds.), 5th Conference: Physics at the LHC 2010, DESY-PROC-2010-01, 2010.
[27] M.G. Albrow, et al., TeV4LHC QCD Working Group, arXiv:hep-ph/0610012.
[28] G. Corcella, et al., J. High Energy Phys. 0101 (2001) 010.
[29] G. Corcella, et al., arXiv:hep-ph/0210213.
[30] T. Kluge, K. Rabbertz, M. Wobisch, arXiv:hep-ph/0609285.
[31] Z. Nagy, Phys. Rev. D 68 (2003) 094002.
[32] Z. Nagy, Phys. Rev. Lett. 88 (2002) 122003.
[33] W.A. Bardeen, A.J. Buras, D.W. Duke, T. Muta, Phys. Rev. D 18 (1978) 3998.
[34] H.L. Lai, et al., Phys. Rev. D 82 (2010) 074024.
[35] R.D. Ball, et al., Nucl. Phys. B 849 (2011) 296.
[36] F. James, Minuit, function minimization and error analysis, CERN Long Writeup D506.
[37] A. Cooper-Sarkar, C. Gwenlan, in: A. De Roeck, H. Jung (Eds.), Proceedings of the Workshop: HERA and the LHC, Part A, Geneva, Switzerland, 2005, CERN-2005-014, DESY-PROC-2005-01, arXiv:hep-ph/0601012, see Part 2, Section 3.
[38] V.M. Abazov, et al., D0 Collaboration, Phys. Rev. D 80 (2009) 111107.
[39] A. Aktas, et al., H1 Collaboration, Phys. Lett. B 653 (2007) 134.
[40] S. Chekanov, et al., ZEUS Collaboration, Phys. Lett. B 649 (2007) 12.
[41] G. Dissertori, et al., J. High Energy Phys. 0908 (2009) 036.
[42] N. Kidonakis, J.F. Owens, Phys. Rev. D 63 (2001) 054019.